Wiley
IET Signal Processing
Volume 2024, Article ID 8852387, 14 pages
https://doi.org/10.1049/2024/8852387

IET The Institution of Engineering and Technology | WILEY

Research Article

Energy Sharing and Performance Bounds in MIMO DFRC Systems: A Trade-Off Analysis

Ziheng Zheng,[1] **Xiang Liu**,[2] **Tianyao Huang**,[3] **Yimin Liu**,[1] **and Yonina C. Eldar**[4]

[1]*Department of Electronic Engineering, Tsinghua University, Beijing 100084, China*
[2]*Institute of Electronic Engineering, China Academy of Engineering Physics, Mianyang, China*
[3]*School of Computer and Communication Engineering, University of Science and Technology Beijing, Beijing 100083, China*
[4]*Faculty of Mathematics and Computer Science, Weizmann Institute of Science, 234 Herzl Street, POB 26, Rehovot 7610001, Israel*

Correspondence should be addressed to Tianyao Huang; huangtianyao@ustb.edu.cn

Received 28 August 2023; Revised 30 May 2024; Accepted 6 August 2024

Academic Editor: Jiahua Zhu

It is a fundamental problem to analyze the performance bound of multiple-input multiple-output dual-functional radar-communication systems. To this end, we derive a performance bound on the communication function under a constraint on radar performance. To facilitate the analysis, in this paper, we consider a simplified situation where there is only one downlink user and one radar target. We analyze the properties of the performance bound and the corresponding waveform design strategy to achieve the bound. When the downlink user and the radar target meet certain conditions, we obtain analytical expressions for the bound and the corresponding waveform design strategy. The results reveal a tradeoff between communication and radar performance, which is essentially caused by the energy sharing and allocation between radar and communication functions of the system.

1. Introduction

With the evolution of radar and wireless communication technology, there is a growing shortage of spectrum resources [1]. To alleviate this problem, many spectrum sharing strategies have been proposed in recent years. These strategies are roughly divided into two categories, i.e., spectrally overlaid systems, wherein radar and communication systems jointly use the same frequency band [2, 3, 4, 5], and dual-functional radar-communication (DFRC) systems, wherein radar and communication are designed in a joint manner [1, 6, 7, 8].

Due to the similarities in both signal processing algorithms and hardware architecture [8, 9], there is a growing demand for implementing radar and communication in one system [1, 6, 7, 8]. To this end, DFRC technology has attracted a lot of attention, as DFRC design reduces system overhead and saves spectrum resources [1, 6, 7]. Among typical DFRC schemes [10, 11, 12, 13], multiple-input multiple-output (MIMO) DFRC is of great significance because of the benefits introduced by transmitting diversity [13, 14, 15]. Therefore, in this paper, we analyze a fundamental performance bound of MIMO DFRC systems.

Many previous works have shown that there are performance tradeoffs between radar and communication in a DFRC system [8, 16, 17]. However, the results are mostly numerical and are achieved under specific signaling and encoding schemes. Just as researchers study channel capacity as a universal performance bound for pure communication systems [18, 19, 20], it is important to find a fundamental performance bound for a MIMO DFRC system.

While it is generally difficult to simultaneously analyze the performance bounds of radar and communication, a common approach in existing works is to calculate the theoretical performance bound of one function while constraining the other [16, 21, 22, 23]. In [21, 23], the radar performance limit is considered under a communication requirement that the downlink user receives the exact desired symbols. Liu et al. [16] and Chen et al. [22] used channel capacity to evaluate the communication performance limit, not restricted to a certain signaling scheme, under some constraints on radar performance. In [21], a simplified single downlink communication user scenario is considered, and an analytical solution to the performance bound is given. However, the strict signaling strategy in [21] causes radar performance degradation. While

in [16, 22, 23], multiuser multitarget scenarios are considered. In such complicated scenarios, the performance bounds are obtained by solving complex optimization problems, and only numerical solutions are obtained.

In this paper, we aim to provide an analytical expression of a fundamental performance bound of a MIMO DFRC system, such that the tradeoff between radar and communication functions is intuitively revealed. To facilitate the analysis, we consider a simplified situation where there is only one downlink user and one radar target. Taking achievable communication rate and radar signal-to-noise ratio (SNR) as the communication and radar performance metrics, respectively, we formulate an optimization problem by constraining the radar SNR and optimizing communication performance. We first theoretically analyze the properties of the optimal solutions to the problem. Then, under some specific situations, i.e., the downlink user has only one receive antenna or the channel matrix and the radar transmit steering vector satisfies certain interrelation, we obtain analytical solutions, which imply an optimal transmit design strategy that achieves the corresponding theoretical performance limit and also offers insight to general MIMO DFRC systems. The main contributions of this work are summarized as follows:

(1) *An optimization for formulating a performance bound on MIMO DFRC systems*. In the simplified situation where there is only one downlink user and one radar target, we formulate the optimization by maximizing the achievable communication rate under the constraint of radar SNR.
(2) *Properties of the optimal solutions*. By theoretically analyzing the optimization, we derive properties the optimal solution satisfies, which offers insights into the optimal beamforming design and guidance for solving the optimization.
(3) *Analytical solutions to the optimization under some specific situations*. Since solving the optimization analytically in general situations is difficult, we derive analytical solutions under the situations where the downlink user has only one receive antenna and where the channel matrix and the radar transmit steering vector satisfy certain interrelation. The optimal solutions imply the optimal transmit designs that achieve the theoretical performance bound of MIMO DFRC systems and show that the optimal transmit designs essentially share and allocate the transmit power between the radar target and the downlink user.

The remainder of this paper is organized as follows: Section 2 introduces the system model and formulates a performance-bound analysis as the optimization problem. Section 3 provides a theoretical analysis to the properties of the optimal solution to the problem. In Section 4, we derive analytical solutions to the optimization problem in the specific situations mentioned above. Simulations are performed to verify the analysis in Section 5. Section 6 draws conclusions.

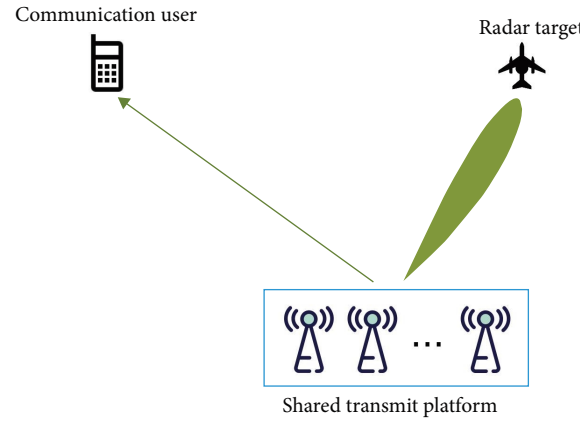

FIGURE 1: System model of a MIMO DFRC system [13].

1.1. Notation. We use boldface lowercase letters for column vectors and boldface uppercase letters for matrices. Superscripts $(\cdot)^H$, $(\cdot)^*$, and $(\cdot)^\dagger$ represent Hermitian transpose, conjugate and Moore–Penrose inverse, respectively, and $\mathrm{tr}(\cdot)$ stands for the trace of a matrix. The N-dimensional complex Euclidean space is expressed as $\mathbb{C}^N$. A complex Gaussian distribution with mean $\boldsymbol{\mu}$ and covariance $\boldsymbol{\Sigma}$ is expressed as $\mathcal{CN}(\boldsymbol{\mu}, \boldsymbol{\Sigma})$. The statistical expectation is represented by $\mathrm{E}[\cdot]$. $|\cdot|$ and $\|\cdot\|_2$ denote absolute value and Euclidean norm, respectively.

2. System Model and Problem Formulation

We consider a theoretical performance bound of a MIMO DFRC system. To this end, we first introduce the system model, the communication and radar performance metrics as well as the transmit power constraint. Then, we formulate the fundamental performance bound as an optimization problem.

A MIMO DFRC system simultaneously performs MIMO communication and MIMO radar functions, whose waveform is optimized to meet the requirements of both radar and communication [6]. To facilitate the theoretical analysis, in this paper, we consider a simplified scenario where there is only one communication user with K receive antennas, one point-like radar target located at angle θ and no clutter, as illustrated in Figure 1. In addition, we assume that the transmit signal is narrow-band, and the system uses the same transmit antennas to receive radar returns. Denote the number of transmit antennas by M. The transmit waveform $\boldsymbol{x} \in \mathbb{C}^M$ is the sum of a series of linear precoded waveforms, given by the following:

$$\boldsymbol{x} = \boldsymbol{W}\boldsymbol{s}, \tag{1}$$

where $\boldsymbol{s} \in \mathbb{C}^N$ represents N orthogonal waveforms and $\boldsymbol{W} \in \mathbb{C}^{M\times N}$ is the precoding matrix to be designed. The orthogonality of the waveforms $\boldsymbol{s}$ means that

$$E[\boldsymbol{s}\boldsymbol{s}^H] = \boldsymbol{I}_N. \tag{2}$$

2.1. Single-User MIMO Communication Performance. The received signal of the communication user $\boldsymbol{y}_C \in \mathbb{C}^K$ is expressed as follows:

$$\boldsymbol{y}_C = \boldsymbol{H}\boldsymbol{x} + \boldsymbol{n}_C, \tag{3}$$

where $\boldsymbol{H} \in \mathbb{C}^{K\times M}$ is the channel matrix, and $\boldsymbol{n}_C \in \mathbb{C}^K$ is additive white Gaussian noise (AWGN) of the communication receiver, i.e., $\boldsymbol{n}_C \sim \mathcal{CN}(\boldsymbol{0}, \sigma^2\boldsymbol{I}_K)$. Without loss of generality, we normalize the power of the AWGN by setting $\sigma^2 = 1$.

The achievable rate is a fundamental bound of communication performance. It is determined by the covariance matrix of the transmit signal, given by the following:

$$\boldsymbol{R} = E[\boldsymbol{x}\boldsymbol{x}^H] = \boldsymbol{W}\boldsymbol{W}^H \in \mathbb{C}^{M\times M}. \tag{4}$$

The achievable rate from the transmitter to the communication user is calculated as follows [18]:

$$C = \log\left|\boldsymbol{I}_K + \boldsymbol{N}_C^{\dagger}\boldsymbol{H}\boldsymbol{R}\boldsymbol{H}^H\right| = \log|\boldsymbol{I}_K + \boldsymbol{H}\boldsymbol{R}\boldsymbol{H}^H|, \tag{5}$$

where $\boldsymbol{N}_C = \mathrm{E}[\boldsymbol{n}_C\boldsymbol{n}_C^H] = \boldsymbol{I}_K$ is the covariance matrix of the AWGN vector $\boldsymbol{n}_C$.

2.2. MIMO Radar Performance. Given target direction θ, the signal impinging on the target is $\boldsymbol{a}_t^H(\theta)\boldsymbol{x}$, where $\boldsymbol{a}_t(\theta) \in \mathbb{C}^M$ is the transmit steering vector. For a uniform linear array (ULA), $\boldsymbol{a}_t$ is given by the following:

$$\boldsymbol{a}_t(\theta) = \left[1 \quad e^{j2\pi\frac{d}{\lambda}\sin\theta} \quad \cdots \quad e^{j2\pi(M-1)\frac{d}{\lambda}\sin\theta}\right]^H, \tag{6}$$

where d is the interval between adjacent antennas and λ is the wavelength. The received signal $\boldsymbol{y}_R \in \mathbb{C}^M$ is expressed as follows:

$$\boldsymbol{y}_R = \alpha_0\boldsymbol{a}_r(\theta)\boldsymbol{a}_t^H(\theta)\boldsymbol{x} + \boldsymbol{n}_R, \tag{7}$$

where α_0 is the target amplitude which is related to the radar cross-section of the target and the path-loss of the signal, $\boldsymbol{a}_r(\theta) \in \mathbb{C}^M$ is the receive steering vector, $\boldsymbol{n}_R \in \mathbb{C}^M$ is the AWGN of the radar receiver, i.e., $\boldsymbol{n}_R \sim \mathcal{CN}(\boldsymbol{0}, \boldsymbol{I}_M)$. We have $\boldsymbol{a}_r(\theta) = \boldsymbol{a}_t(\theta)$ if we use the same antenna array to receive radar returns. We also note that since the radar performance, such as ranging accuracy, is directly related to the SNR, the Doppler frequency and time-delay of the target echo are omitted here for simplicity. The received radar echo is beamformed to enhance the SNR, yielding

$$r = \boldsymbol{w}^H\boldsymbol{y}_R = \alpha_0\boldsymbol{w}^H\boldsymbol{a}_r(\theta)\boldsymbol{a}_t^H(\theta)\boldsymbol{x} + \boldsymbol{w}^H\boldsymbol{n}_R, \tag{8}$$

where $\boldsymbol{w} \in \mathbb{C}^M$ is the receive beamforming vector.

We use SNR to evaluate the radar performance, which is given by Imani et al. [24] as follows:

$$\begin{aligned}\mathrm{SNR} &= E\left[\frac{|\alpha_0\boldsymbol{w}^H\boldsymbol{a}_r(\theta)\boldsymbol{a}_t^H(\theta)\boldsymbol{x}|^2}{|\boldsymbol{w}^H\boldsymbol{n}_R|^2}\right] \\ &= \frac{\alpha_0^2\boldsymbol{w}^H\boldsymbol{a}_r\boldsymbol{a}_t^H\boldsymbol{R}\boldsymbol{a}_t\boldsymbol{a}_r^H\boldsymbol{w}}{\|\boldsymbol{w}\|_2^2}.\end{aligned} \tag{9}$$

Under the constraint $\|\boldsymbol{w}\|_2^2 = 1$, the maximal SNR is achieved when $\boldsymbol{w} = \frac{\boldsymbol{a}_r}{\|\boldsymbol{a}_r\|_2}$. Plugging it into Equation (9), we have the following:

$$\mathrm{SNR} = \alpha_0^2\|\boldsymbol{a}_r\|_2^2\boldsymbol{a}_t^H\boldsymbol{R}\boldsymbol{a}_t. \tag{10}$$

2.3. Transmit Power Constraint. We consider sum-power constraint as follows:

$$E[\|\boldsymbol{x}\|_2^2] \le P, \tag{11}$$

where P is the maximal average transmit power. By substituting Equation (4) into Equation (11), we rewrite the power constraint with respect to $\boldsymbol{R}$ as follows:

$$\mathrm{tr}\,(\boldsymbol{R}) \le P, \tag{12}$$

2.4. Problem Formulation. We formulate the fundamental performance bound of a MIMO DFRC system as an optimization problem. To this end, we calculate the theoretical performance bound of one function while constraining the other. Particularly, in this paper, we calculate the communication capacity under the SNR constraint of the radar function. This yields the optimization problem as follows:

$$\max_{\boldsymbol{R}\succeq\boldsymbol{0}} \ \log|\boldsymbol{I}_K + \boldsymbol{H}\boldsymbol{R}\boldsymbol{H}^H|, \tag{13a}$$

$$\text{s.t. } \alpha_0^2\|\boldsymbol{a}_r\|_2^2\boldsymbol{a}_t^H\boldsymbol{R}\boldsymbol{a}_t \ge \mathrm{SNR}_0, \tag{13b}$$

$$\mathrm{tr}\,(\boldsymbol{R}) \le P, \tag{13c}$$

where SNR_0 is the allowed minimal radar SNR.

Since the radar SNR is directly proportional to $\boldsymbol{a}_t^H\boldsymbol{R}\boldsymbol{a}_t$, which is the power of the signal impinging on the radar target, the constraint (Equation (13b)) can be rewritten as $\boldsymbol{a}_t^H\boldsymbol{R}\boldsymbol{a}_t \ge \frac{\mathrm{SNR}_0}{\alpha_0^2\|\boldsymbol{a}_r\|_2^2} = \gamma$, where γ is the minimal power impinging on the radar target. In addition, since larger transmit power always leads to higher channel capacity, we let the sum-power constraint (Equation (13c)) hold with equality. Therefore, Equation (13) is equivalently expressed as follows:

$$\max_{\boldsymbol{R}\succeq\boldsymbol{0}} \ \log|\boldsymbol{I}_K + \boldsymbol{H}\boldsymbol{R}\boldsymbol{H}^H|, \tag{14a}$$

$$\text{s.t. } \boldsymbol{a}_t^H\boldsymbol{R}\boldsymbol{a}_t \ge \gamma, \tag{14b}$$

$$\mathrm{tr}\,(\boldsymbol{R}) = P. \tag{14c}$$

Note that Equation (14a) is a logdet function, which is concave, Equations (14b) and (14c) are linear; hence, the

optimization problem (Equation (14)) is convex. By solving Equation (14), we obtain the channel capacity and the corresponding waveform $\boldsymbol{R}=\boldsymbol{W}\boldsymbol{W}^H$ to achieve it.

3. Properties of the Optimal Transmit Covariance Matrix

Consider the eigenvalue decomposition of the transmit covariance matrix as follows:

$$\boldsymbol{R}=\boldsymbol{U}\Lambda\boldsymbol{U}^H=\sum_{i=1}^{r}\lambda_i\boldsymbol{u}_i\boldsymbol{u}_i^H=\sum_{i=1}^{r}\boldsymbol{v}_i\boldsymbol{v}_i^H=\boldsymbol{V}\boldsymbol{V}^H, \tag{15}$$

where $\boldsymbol{v}_i=\sqrt{\lambda_i}\boldsymbol{u}_i$ $(i=1,2,\cdots,r)$, $\boldsymbol{V}\in\mathbb{C}^{M\times r}$, and r is the rank of $\boldsymbol{R}$. Combining Equation (15) with Equation (4), let $\boldsymbol{W}=\boldsymbol{V}$, we see that the rank of $\boldsymbol{R}$ denotes the number of orthogonal waveforms needed and the eigenvectors of $\boldsymbol{R}$ are closely related to the linear precoding scheme. Besides, in general situations, it is difficult to obtain an analytical solution to Equation (14). Hence, in this section, we conduct a preliminary analysis of Equation (14) to find out some properties of the optimal transmit covariance matrix, which help us solve Equation (14) analytically in some specific situations and provide insights into the optimal beamforming design.

Proposition 1. *The rank of the optimal transmit covariance matrix* $\boldsymbol{R}$ *and the rank of the channel matrix* $\boldsymbol{H}$ *satisfy that*

$$\operatorname{rank}(\boldsymbol{R})\le\operatorname{rank}(\boldsymbol{H})+1. \tag{16}$$

Proof. Inspired by the analysis in [20], we start with the Karush–Kuhn–Tucker (KKT) conditions of Equation (14). The Lagrange function of the optimization problem is given by the following:

$$\begin{aligned}L(\boldsymbol{R},\lambda,\mu)=&-\log|\boldsymbol{I}+\boldsymbol{H}\boldsymbol{R}\boldsymbol{H}^H|+\lambda(\gamma-\boldsymbol{a}_t^H\boldsymbol{R}\boldsymbol{a}_t)\\&+\mu(\operatorname{tr}(\boldsymbol{R})-P),\end{aligned} \tag{17}$$

where λ and μ are dual variables. The KKT conditions of Equation (14) imply that

$$\nabla L(\boldsymbol{R},\lambda,\mu)=\boldsymbol{0}, \tag{18}$$

where

$$\nabla L(\boldsymbol{R},\lambda,\mu)=-\boldsymbol{H}^H(\boldsymbol{I}+\boldsymbol{H}\boldsymbol{R}\boldsymbol{H}^H)^{-1}\boldsymbol{H}-\lambda\boldsymbol{a}_t\boldsymbol{a}_t^H+\mu\boldsymbol{I}. \tag{19}$$

By multiplying both sides of Equation (18) on the right with $\boldsymbol{R}$ we have the following:

$$-\boldsymbol{H}^H(\boldsymbol{I}+\boldsymbol{H}\boldsymbol{R}\boldsymbol{H}^H)^{-1}\boldsymbol{H}\boldsymbol{R}=(\lambda\boldsymbol{a}_t\boldsymbol{a}_t^H-\mu\boldsymbol{I})\boldsymbol{R}. \tag{20}$$

When $\lambda\neq\frac{\mu}{\|\boldsymbol{a}_t\|^2}$, $\lambda\boldsymbol{a}_t\boldsymbol{a}_t^H-\mu\boldsymbol{I}$ is invertible. According to Equation (20), we have the following:

$$\begin{aligned}\operatorname{rank}(\boldsymbol{R})&=\operatorname{rank}((\lambda\boldsymbol{a}_t\boldsymbol{a}_t^H-\mu\boldsymbol{I})\boldsymbol{R})\\&=\operatorname{rank}(-\boldsymbol{H}^H(\boldsymbol{I}+\boldsymbol{H}\boldsymbol{R}\boldsymbol{H}^H)^{-1}\boldsymbol{H}\boldsymbol{R})\\&\le\operatorname{rank}(\boldsymbol{H}).\end{aligned} \tag{21}$$

When $\lambda=\frac{\mu}{\|\boldsymbol{a}_t\|^2}$, since

$$\begin{cases}(\lambda\boldsymbol{a}_t\boldsymbol{a}_t^H-\mu\boldsymbol{I})\boldsymbol{a}_t=\boldsymbol{0},\\(\lambda\boldsymbol{a}_t\boldsymbol{a}_t^H-\mu\boldsymbol{I})\boldsymbol{u}=-\mu\boldsymbol{u},\forall\boldsymbol{u}\in\mathbb{C}^M,\boldsymbol{a}_t^H\boldsymbol{u}=0,\end{cases} \tag{22}$$

$\lambda\boldsymbol{a}_t\boldsymbol{a}_t^H-\mu\boldsymbol{I}$ is a singular matrix whose rank is $M-1$. According to the Sylvester inequality, we have the following:

$$\begin{aligned}&\operatorname{rank}((\lambda\boldsymbol{a}_t\boldsymbol{a}_t^H-\mu\boldsymbol{I})\boldsymbol{R})\\&\ge\operatorname{rank}(\lambda\boldsymbol{a}_t\boldsymbol{a}_t^H-\mu\boldsymbol{I})+\operatorname{rank}(\boldsymbol{R})-M\\&=\operatorname{rank}(\boldsymbol{R})-1.\end{aligned} \tag{23}$$

Thereby,

$$\begin{aligned}\operatorname{rank}(\boldsymbol{R})&\le\operatorname{rank}((\lambda\boldsymbol{a}_t\boldsymbol{a}_t^H-\mu\boldsymbol{I})\boldsymbol{R})+1\\&=\operatorname{rank}(-\boldsymbol{H}^H(\boldsymbol{I}+\boldsymbol{H}\boldsymbol{R}\boldsymbol{H}^H)^{-1}\boldsymbol{H}\boldsymbol{R})+1\\&\le\operatorname{rank}(\boldsymbol{H})+1.\end{aligned} \tag{24}$$

From the analysis above, we see that the rank of the optimal transmit covariance matrix must be no more than the rank of the channel matrix plus 1, and equality can be obtained only when the dual variables satisfy the equation $\lambda=\frac{\mu}{\|\boldsymbol{a}_t\|^2}$. □

Furthermore, when the transmit steering vector $\boldsymbol{a}_t$ is orthogonal to the row space of the channel matrix $\boldsymbol{H}$, which means $\boldsymbol{H}\boldsymbol{a}_t=\boldsymbol{0}$, we have the following:

$$(\lambda\boldsymbol{a}_t^H\boldsymbol{a}_t\boldsymbol{a}_t^H-\mu\boldsymbol{a}_t^H)\boldsymbol{R}=(\lambda\|\boldsymbol{a}_t\|^2-\mu)\boldsymbol{a}_t^H\boldsymbol{R}=\boldsymbol{0}, \tag{25}$$

by multiplying both sides of Equation (20) on the left with $\boldsymbol{a}_t^H$. According to the radar SNR constraint (Equation (14b)), $\boldsymbol{a}_t^H\boldsymbol{R}\neq0$, therefore $\lambda\|\boldsymbol{a}_t\|^2-\mu=0$, $\lambda=\frac{\mu}{\|\boldsymbol{a}_t\|^2}$. That is to say, when $\boldsymbol{a}_t$ is orthogonal to the row space of $\boldsymbol{H}$, there may exist an optimal transmit covariance matrix $\boldsymbol{R}$ that satisfies $\operatorname{rank}(\boldsymbol{R})=\operatorname{rank}(\boldsymbol{H})+1$.

Proposition 2. *There always exists an optimal transmit covariance matrix* $\boldsymbol{R}$ *whose rank equals the rank of the channel matrix* $\boldsymbol{H}$.

Proof. To illustrate this point, we first consider the following optimization problem:

$$\max_{\boldsymbol{R}\succeq\boldsymbol{0}}\ \log|\boldsymbol{I}_K+\boldsymbol{H}\boldsymbol{R}\boldsymbol{H}^H|, \tag{26a}$$

$$\text{s.t. }\operatorname{tr}(\boldsymbol{Q}_i\boldsymbol{R})=P_i\ \ (i=1,2,\cdots,n), \tag{26b}$$

where $\boldsymbol{Q}_i$ $(i=1,2,\cdots,n)$ are given Hermitian matrices and the rank of $\boldsymbol{H}$ is k. □

Theorem 1. *If the feasible set of the optimization variable $\boldsymbol{R}$ in Equation (26) is nonempty, bounded, and closed, there must be an optimal solution whose rank is no more than r, where r satisfies as follows:*

$$r^2 \le k^2 + n < (r+1)^2. \tag{27}$$

Furthermore, if we change some of the equality constraints to inequality constraints, the result will still be true.

The proof is given in Appendix A.

As for the optimization problem (Equation (14)), rewrite the constraints (Equations (14b) and (14c)) as $\mathrm{tr}(\boldsymbol{a}_t\boldsymbol{a}_t^H\boldsymbol{R}) \ge \gamma$ and $\mathrm{tr}(\boldsymbol{I}\boldsymbol{R}) = P$, respectively. Thus, Equation (14) is expressed in the form of Equation (26) with $n = 2$. According to Theorem 1, Equation (14) has an optimal solution whose rank is no more than r, where r satisfies $r^2 \le k^2 + 2 < (r+1)^2$. Since r, $k \in \mathbb{Z}^+$, we obtain that $r = k$, which means that there is always an optimal transmit covariance matrix whose rank equals to the rank of the channel matrix.

Proposition 3. *The eigenvectors of the optimal transmit covariance matrix $\boldsymbol{R}$ are linear combinations of the channel matrix $\boldsymbol{H}$ and the transmit steering vector $\boldsymbol{a}_t$.*

Proof. Since the transmit covariance matrix $\boldsymbol{R}$ is semidefinite, assume that

$$\boldsymbol{R} = \boldsymbol{C}\boldsymbol{C}^H, \tag{28}$$

where $\boldsymbol{C} \in \mathbb{C}^{M\times M}$ is an arbitrary $M \times M$ matrix, whose column space is the same as the column space of $\boldsymbol{R}$.

By substituting Equation (28) into Equation (14), we rewrite the optimization problem as follows:

$$\max_{\boldsymbol{C}} \ \log|\boldsymbol{I}_K + \boldsymbol{H}\boldsymbol{C}\boldsymbol{C}^H\boldsymbol{H}^H|, \tag{29a}$$

$$\text{s.t. } \boldsymbol{a}_t^H\boldsymbol{C}\boldsymbol{C}^H\boldsymbol{a}_t \ge \gamma, \tag{29b}$$

$$\mathrm{tr}(\boldsymbol{C}\boldsymbol{C}^H) = P. \tag{29c}$$

The Lagrange function of Equation (29) is given by the following:

$$\begin{aligned} L(\boldsymbol{C}, \boldsymbol{C}^*, \lambda, \mu) = &- \log|\boldsymbol{I} + \boldsymbol{H}\boldsymbol{R}\boldsymbol{H}^H| + \lambda(\gamma - \boldsymbol{a}_t^H\boldsymbol{R}\boldsymbol{a}_t) \\ &+ \mu(\mathrm{tr}(\boldsymbol{R}) - P), \end{aligned} \tag{30}$$

where $\boldsymbol{R} = \boldsymbol{C}\boldsymbol{C}^H$, λ and μ are dual variables. According to the KKT conditions, the gradient of the Lagrange function equals zero.

$$\begin{aligned} &\frac{\partial L(\boldsymbol{C}, \boldsymbol{C}^*, \lambda, \mu)}{\partial \boldsymbol{C}^*} \\ &= -\boldsymbol{H}^H(\boldsymbol{I} + \boldsymbol{H}\boldsymbol{C}\boldsymbol{C}^H\boldsymbol{H}^H)^{-1}\boldsymbol{H}\boldsymbol{C} - \lambda\boldsymbol{a}_t\boldsymbol{a}_t^H\boldsymbol{C} + \mu\boldsymbol{C} \\ &= \boldsymbol{0}. \end{aligned} \tag{31}$$

Rewrite Equation (31) as follows:

$$\begin{aligned} \boldsymbol{C} &= \frac{1}{\mu}\boldsymbol{H}^H(\boldsymbol{I} + \boldsymbol{H}\boldsymbol{C}\boldsymbol{C}^H\boldsymbol{H}^H)^{-1}\boldsymbol{H}\boldsymbol{C} + \frac{\lambda}{\mu}\boldsymbol{a}_t\boldsymbol{a}_t^H\boldsymbol{C} \\ &= \frac{1}{\mu}\boldsymbol{H}^H\boldsymbol{X} + \frac{\lambda}{\mu}\boldsymbol{a}_t\boldsymbol{Y}, \end{aligned} \tag{32}$$

where $\boldsymbol{X} = (\boldsymbol{I} + \boldsymbol{H}\boldsymbol{C}\boldsymbol{C}^H\boldsymbol{H}^H)^{-1}\boldsymbol{H}\boldsymbol{C}$ and $\boldsymbol{Y} = \boldsymbol{a}_t^H\boldsymbol{C}$.

From Equation (32), we see that the columns of $\boldsymbol{C}$ belong to the linear space spanned by the columns of $\boldsymbol{H}^H$ and $\boldsymbol{a}_t$. Thus, the eigenvectors of the optimal transmit covariance matrix $\boldsymbol{R}$ are linear combinations of the channel matrix $\boldsymbol{H}$ and the transmit steering vector $\boldsymbol{a}_t$. □

4. Optimal Transmit Beamforming in Particular Cases

By utilizing the properties provided in Section 3, we can solve the optimization problem (Equation (14)) analytically under particular situations. In this section, we consider two particular situations, offering insights into the MIMO DFRC system.

4.1. Single-Antenna Downlink User. Consider the case where the communication user has only one receive antenna, i.e., $K = 1$. In this situation, the channel matrix becomes a row vector:

$$\boldsymbol{H} = \boldsymbol{h}^H, \tag{33}$$

where $\boldsymbol{h}$ is referred to as the channel vector. Accordingly, the objective function (Equation (14a)) becomes the following:

$$\log(1 + \boldsymbol{h}^H\boldsymbol{R}\boldsymbol{h}). \tag{34}$$

Since the value of Equation (34) monotonically increases with $\boldsymbol{h}^H\boldsymbol{R}\boldsymbol{h}$, which is the power of the signal transmitted to the communication user, maximizing Equation (34) is equivalent to maximizing $\boldsymbol{h}^H\boldsymbol{R}\boldsymbol{h}$. Therefore, in this situation, we rewrite the optimization problem as follows:

$$\max_{\boldsymbol{R}\succeq\boldsymbol{0}} \ \boldsymbol{h}^H\boldsymbol{R}\boldsymbol{h}, \tag{35a}$$

$$\text{s.t. } \boldsymbol{a}_t^H\boldsymbol{R}\boldsymbol{a}_t \ge \gamma, \tag{35b}$$

$$\mathrm{tr}(\boldsymbol{R}) = P. \tag{35c}$$

4.1.1. Optimal Beamforming Design. According to Propositions 2 and 3, there is an optimal solution whose rank is no

more than 1, and its eigenvector is a linear combination of $\boldsymbol{h}$ and $\boldsymbol{a}_t$. Thus, we assume that

$$\boldsymbol{R} = \boldsymbol{c}\boldsymbol{c}^H, \tag{36}$$

$$\boldsymbol{c} = a\boldsymbol{h} + b\boldsymbol{a}_t, \tag{37}$$

where $\boldsymbol{c} \in \mathbb{C}^M$ and $a, b \in \mathbb{C}$. Substituting Equation (36) into Equation (35) yields the following:

$$\max_{\boldsymbol{C}} \ |\boldsymbol{c}^H\boldsymbol{h}|^2, \tag{38a}$$

$$\text{s.t.} \ |\boldsymbol{c}^H\boldsymbol{a}_t|^2 \geq \gamma, \tag{38b}$$

$$\boldsymbol{c}^H\boldsymbol{c} = P. \tag{38c}$$

Solving the KKT conditions of Equation (38), we find that

(i) When $0 \leq \gamma < \frac{P|\boldsymbol{h}^H\boldsymbol{a}_t|^2}{\|\boldsymbol{h}\|_2^2}$,

$$\begin{cases} |a| = \dfrac{\sqrt{P}}{\|\boldsymbol{h}\|_2}, \\ |b| = 0, \end{cases} \tag{39}$$

where the phase of a is arbitrary.

(ii) When $\frac{P|\boldsymbol{h}^H\boldsymbol{a}_t|^2}{\|\boldsymbol{h}\|_2^2} \leq \gamma \leq P\|\boldsymbol{a}_t\|_2^2$,

$$\begin{cases} |a| = \eta, \\ |b| = \dfrac{\sqrt{\gamma}}{\|\boldsymbol{a}_t\|_2^2} - \dfrac{|\boldsymbol{h}^H\boldsymbol{a}_t|}{\|\boldsymbol{a}_t\|_2^2}\eta, \end{cases} \tag{40}$$

where

$$\eta = \sqrt{\frac{P\|\boldsymbol{a}_t\|_2^2 - \gamma}{\|\boldsymbol{h}\|_2^2\|\boldsymbol{a}_t\|_2^2 - |\boldsymbol{h}^H\boldsymbol{a}_t|^2}}, \tag{41}$$

and the phases of a and b should satisfy as follows:

$$\arg(a) - \arg(b) = \arg(\boldsymbol{h}^H\boldsymbol{a}_t), \tag{42}$$

if $\boldsymbol{h}^H\boldsymbol{a}_t \neq 0$ or can be arbitrary if $\boldsymbol{h}^H\boldsymbol{a}_t = 0$.

(iii) When $\gamma > P\|\boldsymbol{a}_t\|_2^2$, there is no feasible solution.

The derivation is provided in Appendix B.

The formation of $\boldsymbol{c}$ indicates that the design of the optimal waveform is actually power allocation between the radar target and the communication user. The coefficients a and b represent the amplitudes of resources allocated for communication and radar sensing, respectively. In case (i), the requirement for the radar sensing SNR is low and $|b| = 0$. In this case, we do not need to particularly allocate power to the radar target, as the signal transmitted to the communication user already sheds enough power on the radar target to meet the SNR requirement. In case (ii), the requirement for the radar sensing SNR is higher. In this case, as the SNR requirement increases, γ increases, thereby $|a|$ decreases and $|b|$ increases, which means that we need to allocate more power to radar sensing. When $\gamma = P\|\boldsymbol{a}_t\|_2^2$, $|a| = 0$, the multi-antenna transmitter works like a phased-array radar and the radar SNR achieves its upper bound. In case (iii), there is no feasible solution, since we can only achieve limited radar SNR with limited transmit power.

When the radar target and the communication user are in the same direction, which means that $\boldsymbol{a}_t$ is parallel to $\boldsymbol{h}$, the communication waveform also serves as the radar sensing waveform, and there is no need to allocate the transmit power. When $\boldsymbol{a}_t$ is orthogonal to $\boldsymbol{h}$, radar sensing and communication functions operate independently without any energy sharing between each other. The expressions of the power allocated for communication and radar sensing are $|a|^2\|\boldsymbol{h}\|_2^2$ and $|b|^2\|\boldsymbol{a}_t\|_2^2$, respectively, which satisfy the equation $|a|^2\|\boldsymbol{h}\|_2^2 + |b|^2\|\boldsymbol{a}_t\|_2^2 = P$.

4.1.2. Channel Capacity Analysis. By substituting the optimal solution $\boldsymbol{R}$ into Equation (34), we obtain the channel capacity with respect to radar SNR threshold γ as follows:

(i) When $0 \leq \gamma < \frac{P|\boldsymbol{h}^H\boldsymbol{a}_t|^2}{\|\boldsymbol{h}\|_2^2}$,

$$C = \log(1 + P\|\boldsymbol{h}\|_2^2). \tag{43}$$

The channel capacity is constant.

(ii) When $\frac{P|\boldsymbol{h}^H\boldsymbol{a}_t|^2}{\|\boldsymbol{h}\|_2^2} \leq \gamma \leq P\|\boldsymbol{a}_t\|_2^2$,

$$C = \log\left(1 + \frac{\left(\sqrt{\gamma}|\boldsymbol{h}^H\boldsymbol{a}_t| + \sqrt{\beta}\right)^2}{\|\boldsymbol{a}_t\|_2^4}\right), \tag{44}$$

where

$$\beta = (P\|\boldsymbol{a}_t\|_2^2 - \gamma)(\|\boldsymbol{h}\|_2^2\|\boldsymbol{a}_t\|_2^2 - |\boldsymbol{h}^H\boldsymbol{a}_t|^2). \tag{45}$$

(iii) When $\gamma > P\|\boldsymbol{a}_t\|_2^2$, the transmit power is not enough to meet the radar SNR requirement.

In case (i), since there is no dedicated radar signal (the communication signal simultaneously serves as a probing function), the channel capacity is constant and equals the achievable capacity of the pure MIMO communication system without radar function. In case (ii), we see that $\frac{\partial C}{\partial \gamma} \leq 0$,

which means the channel capacity is negatively correlated with the threshold γ, which indicates the performance trade-off between radar sensing and communication.

4.2. Multiantenna Downlink User with Specific Relationships between the Channel Matrix and the Transmit Steering Vector. Although it is difficult to solve Equation (14) analytically in general situations, the analytical solution is acquirable when the channel matrix $\boldsymbol{H}$ and the transmit steering vector $\boldsymbol{a}_t$ satisfy certain relationships, i.e., $\boldsymbol{a}_t$ is either parallel to one of the right-singular vectors of $\boldsymbol{H}$ or orthogonal to the row space of $\boldsymbol{H}$.

In these two cases, we find that the eigenvectors of the optimal transmit covariance matrix $\boldsymbol{R}$ are parallel to the right-singular vectors of $\boldsymbol{H}$ and $\boldsymbol{a}_t$. The corresponding eigenvalues are chosen to meet the radar SNR constraint (Equation (14b)) first, and the rest of them are determined by using water-filling algorithm [25] under the sum-power constraint (Equation (14c)) (the specific derivation is provided in Appendix C).

Since the eigenvalues of $\boldsymbol{R}$ denote the transmit power, this result reflects the power allocation between radar and communication in MIMO DFRC systems.

5. Numerical Results

In this section, we demonstrate the performance of MIMO DFRC systems via numerical simulations.

Under the situation of a single-antenna downlink communication user, we consider a ULA transmitter with half-wavelength element spacing $d = \frac{\lambda}{2}$ and the number of the transmit antennas $M = 10$. The radar target is located at angle θ. The communication signal is transmitted directly from the transmitter to the communication user. Given the communication user direction θ_C, the channel vector $\boldsymbol{h}$ is given by the following:

$$\boldsymbol{h} = \left[1 \quad e^{j\pi \sin\theta_C} \quad \cdots \quad e^{j9\pi \sin\theta_C}\right]^H. \tag{46}$$

In the simulation, we use SNR loss to represent the SNR threshold in Equation (13), given by the following:

$$\text{SNR loss} = 10\log_{10}\left(\frac{\text{SNR}_0}{\text{SNR}_{\text{MAX}}}\right), \tag{47}$$

where $\text{SNR}_{\text{MAX}} = \alpha_0^2 \|\boldsymbol{a}_r\|_2^2 P \|\boldsymbol{a}_t\|_2^2$ is the maximal achievable SNR under the sum-power constraint.

We perform the first simulation to demonstrate the channel capacity versus radar SNR loss with θ set to $-30°$ and θ_C set to $-30°$, 0°, and 30°. The transmit SNR $P/\sigma^2 =$ 13 dB. The results are shown in Figure 2. Since both Equations (13) and (14) are convex and can be solved by the CVX, a package for specifying and solving convex programs [26, 27], we also compare the analytical expressions of the optimal solutions given in Section 4.1 with the CVX results, denoted by "analytical" and "CVX," respectively. We find that for the same θ_C, the CVX and analytical expressions yield the same curve, verifying the correctness of the derivation in Section 4.1.

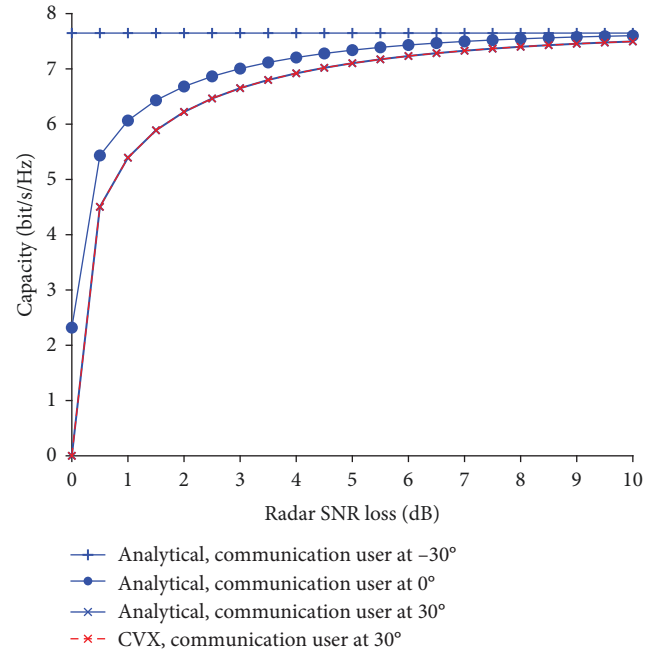

FIGURE 2: Channel capacity versus radar SNR loss (single-antenna downlink user).

From Figure 2, the channel capacity increases with the radar SNR loss when the communication user and the radar target are in different directions, $\theta \neq \theta_C$, while the capacity is fixed when $\theta = \theta_C$. We explain the phenomenon under different locations of single-antenna downlink users and targets.

(1) When $\theta = -30°$ and $\theta_C = 30°$, it holds that $\boldsymbol{h}^H \boldsymbol{a}_t = 0$. In this case, there is no energy sharing between radar and communication functions. As a result, which is the channel capacity reduces to 0 when the radar SNR loss is 0, because all the transmit energy is allocated to the radar. As the radar SNR loss becomes higher, the channel capacity increases and reaches its upper bound, which is the channel capacity of a communication-only system with all the transmit power allocated to communication.

(2) When $\theta = \theta_C$, which means that $\boldsymbol{a}_t$ is parallel to $\boldsymbol{h}$, the transmit power is shared between these two functions. Consequently, by allocating all the transmit power in the desired direction, the channel capacity is fixed and achieves the upper bound, and the radar SNR is maximized simultaneously.

(3) When $\theta_C = 0°$, the steering vector $\boldsymbol{a}_t$ is neither parallel nor perpendicular to $\boldsymbol{h}$. Part of the transmit power for communication is also used for probing. Therefore, even when the SNR loss is strictly 0, the capacity is still positive. The capacity curve stays between those of $\theta_C = -30°$ and 30°.

In the second simulation, we show the transmit beam patterns for different radar SNR losses in Figures 3(a) and 3(b), where θ is set to $-30°$, θ_C is set to $-30°$ and 0°,

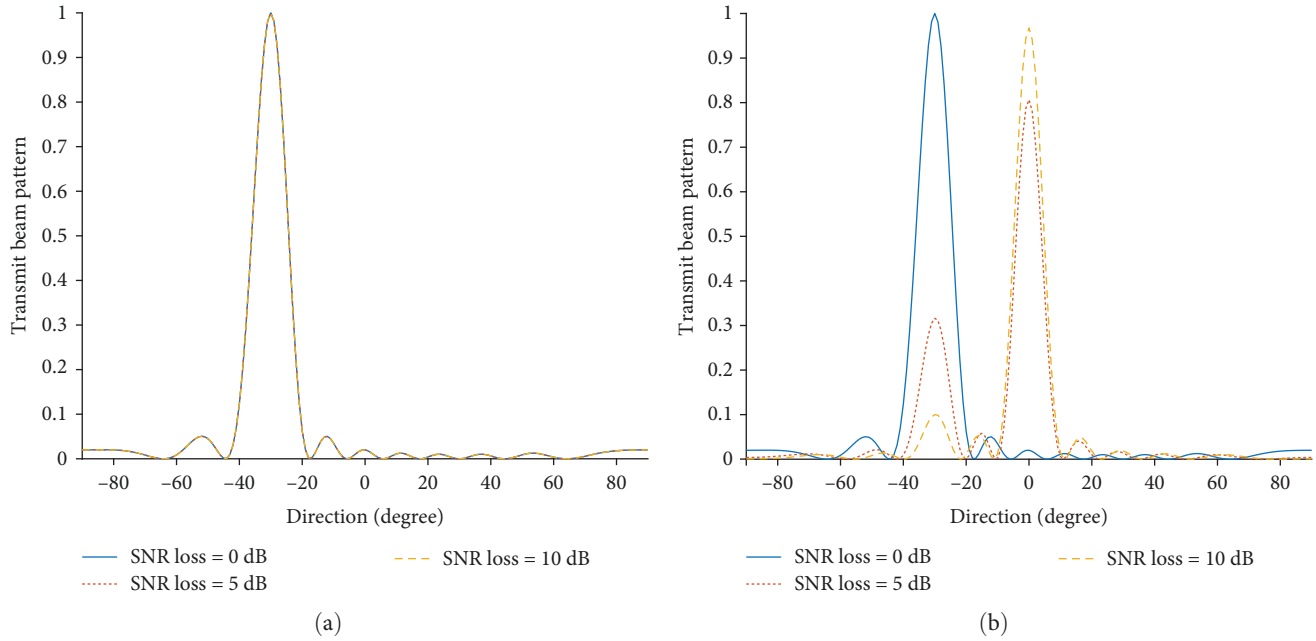

FIGURE 3: Transmit beam pattern for different SNR loss (single-antenna downlink user): (a) radar target at −30°, communication user at −30°; (b) radar target at −30°, communication user at 0°.

respectively. The beam patterns are normalized to the peak value of the one obtained under 0 dB radar SNR loss. In Figure 3(a), when the communication user and radar target are in the same direction, $\theta = \theta_C$, the transmit beam pattern is toward θ for different radar SNR losses. In this case, there is no power allocation between radar and communication, because the communication signal simultaneously serves for probing. In Figure 3(b), when $\theta \neq \theta_C$, there are two beams towards θ and θ_C, respectively, indicating that the transmit power is allocated between radar and communication functions. As the radar SNR loss increases, less power is allocated to the radar target.

Our third simulation verifies the achievability of the performance bound by calculating the bit error rate (BER) of communication using the proposed beamforming design. We use a low-density parity-check (LDPC) code [28] whose rate is 3/4, block length is 3, 240, and a 64-QAM modulation. Thus, the rate of communication is 4.5 bits/s/Hz. According to Figure 2, the rate is achieved when the radar target is located at $\theta = -30°$, the communication user is located at $\theta_C = 30°$ and radar SNR loss is 0.5 dB. We obtain the precoding matrix under this condition using the results in Section 4.1.1. The relationship between BER and transmit SNR is shown in Figure 4. From Figure 4, we see that as the transmit SNR increases, the BER correspondingly decreases. When the transmit SNR achieves 16 dB, the BER becomes less than 10^{-6}. Since the results in Figure 2 are achieved under the condition that the transmit SNR is 13 dB, our proposed beamforming design is about 3 dB from the capacity limit. The gap is mainly caused by the performance of the LDPC code we use.

We demonstrate the communication BER and the radar pulse compression performance with respect to different directions of communication user and radar target in our

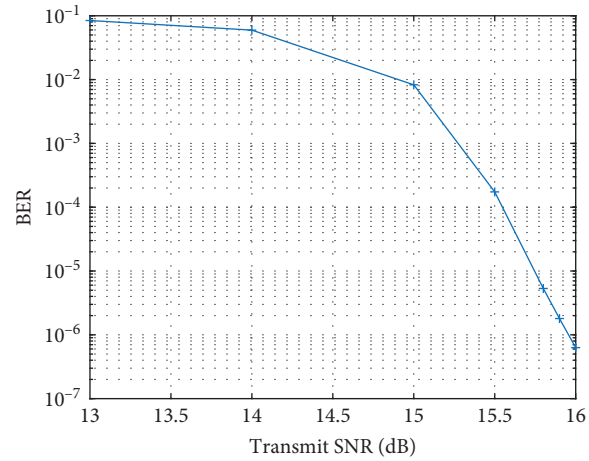

FIGURE 4: BER versus transmit SNR.

fourth simulation. We set the transmit SNR P/σ^2 to 13 dB, radar SNR loss to 3 dB, and the direction of radar target θ to $-30°$. Figure 5(a) shows the relationship between the BER of communication and the direction of the downlink user using the proposed beamforming design. For communication, we use an LDPC code [28] whose rate is 5/6, block length is 648, and a 64-QAM modulation. As shown in Figure 5(a), the BER is related to the relationship between $\boldsymbol{h}$ and $\boldsymbol{a}_t$. In particular, when θ_C is around θ, the BER achieves its minimum. The relationship between the amplitude of radar pulse compression and the direction of the downlink user is shown in Figure 5(b). We see that when θ_C is around θ, the radar pulse compression amplitude achieves the maximum value. Otherwise, the amplitude is constant due to the constraint on radar SNR. Since $\boldsymbol{h}$ and $\boldsymbol{a}_t$ are nearly parallel to each other

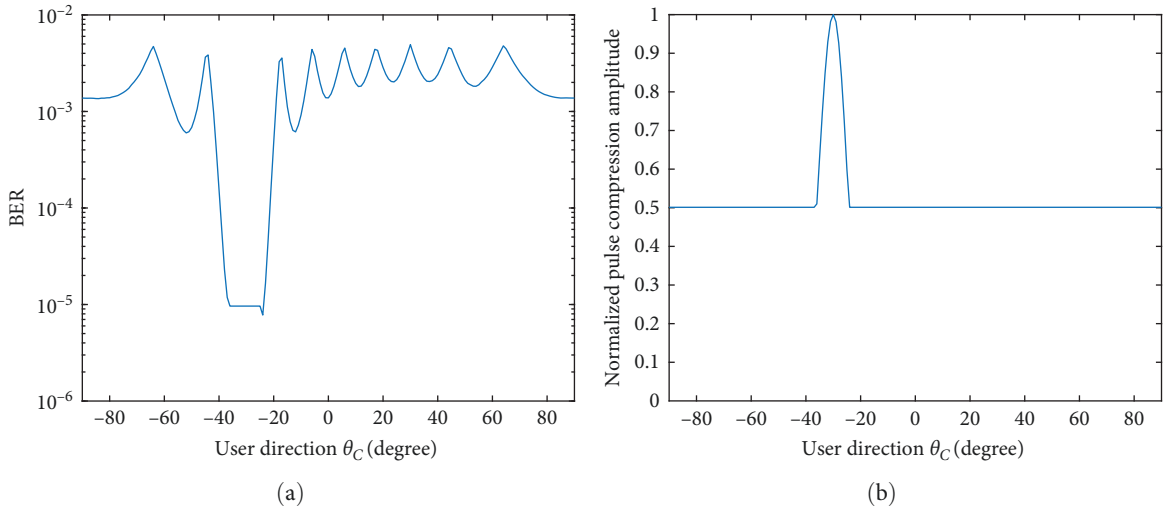

FIGURE 5: The communication BER and the radar pulse compression performance with respect to different downlink user's directions: (a) BER versus θ_C; (b) normalized radar pulse compression amplitude versus θ_C.

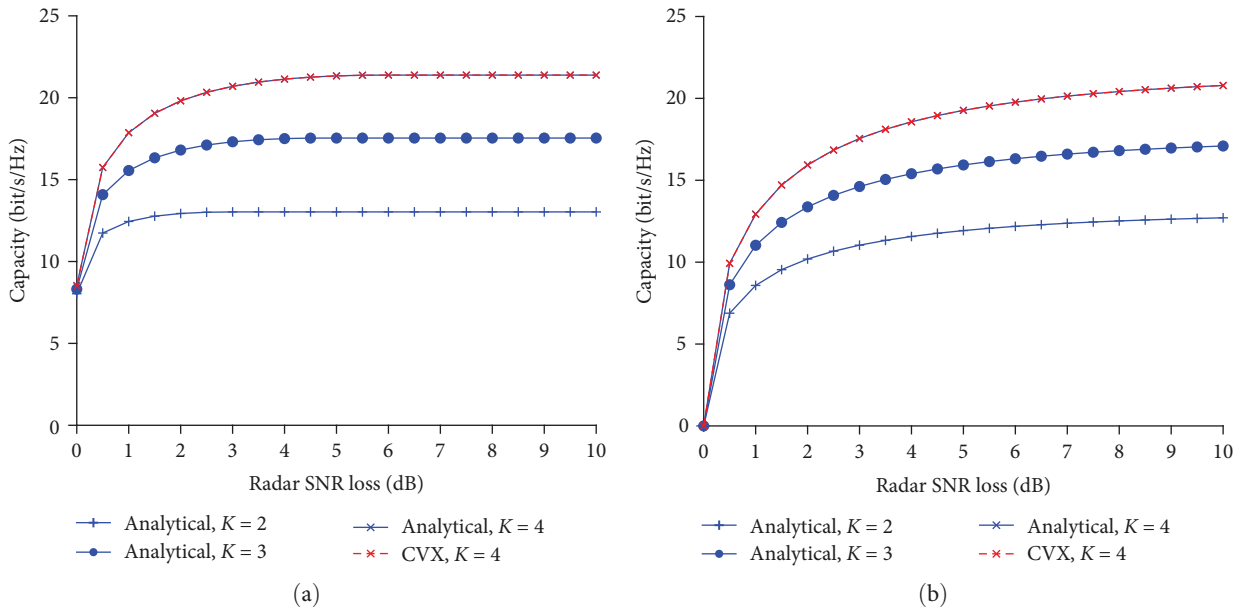

FIGURE 6: Channel capacity versus radar SNR loss (multi-antenna downlink user): (a) $\boldsymbol{a}_t$ parallel to one of the right-singular vectors of $\boldsymbol{H}$; (b) $\boldsymbol{a}_t$ orthogonal to the row space of $\boldsymbol{H}$.

when θ_C is around θ, most of the transmit power is shared between radar and communication. As a result, the optimal communication performance and the radar SNR constraint are achieved at the same time.

We note that our results are different from those in [21], which states that there is SNR loss for radar when the communication user and the radar target are in the same direction. The reason is that in this paper, we use the capacity to evaluate the communication performance, not restricting to using a certain coding strategy for communication. However, the signaling scheme in [21] constrains that the downlink user receives desired signals, which causes SNR loss for radar.

Under the situation of a multiantenna downlink communication user, we consider a transmitter with $M = 10$ antennas and a communication user with $K = 2, 3, 4$ antennas, respectively. The transmit SNR P/σ^2 is 13 dB. The communication channel is Rayleigh fading, i.e., the entries of $\boldsymbol{H}$ obey independent standard complex normal distribution. The transmit steering vector $\boldsymbol{a}_t$ is set either parallel to one of the right-singular vectors of $\boldsymbol{H}$ or orthogonal to the row space of $\boldsymbol{H}$.

We perform the fifth simulation to demonstrate the relation between the channel capacity and the radar SNR loss when the communication user has multiple receive antennas. The results are shown in Figure 6. The analytical solution

TABLE 1: Runtime of solving the optimization.

Number of receive antennas	CVX	Analytical solution
$K=1$	0.915 s	3.64×10^{-5} s
$K=4$	1.40 s	2.44×10^{-4} s

given in Section 4.2 is compared with the CVX results when $K=4$, denoted by "analytical, $K=4$" and "CVX, $K=4$" in Figure 6, respectively.

From Figure 6, the channel capacity increases with radar SNR loss, and the number of communication user's receive antennas. We note that there are some differences and similarities in Figures 6(a) and 6(b), which are explained in the following discussion.

(1) When $\boldsymbol{a_t}$ is parallel to one of the right-singular vectors of $\boldsymbol{H}$, there is energy sharing between radar and communication. The amount of energy shared depends on the corresponding singular value of $\boldsymbol{H}$. Thus, even when the radar SNR loss achieves 0, the capacity is still positive, and when radar SNR loss is high enough, the capacity achieves a maximum value, which is the channel capacity of a communication-only system with all the transmit power allocated to communication.
(2) When $\boldsymbol{a_t}$ is orthogonal to the row space of $\boldsymbol{H}$, there is no energy sharing between radar and communication. Therefore, when the radar SNR loss is 0, the channel capacity reduces to 0 at the same time. The maximum value of capacity is achieved only when the radar SNR reaches 0.
(3) In both situations, when radar SNR loss achieves 0, the capacity is almost identical regardless of K. This is because when radar SNR loss is low, the transmit energy is mainly allocated to radar. And when radar SNR loss is high, the maximum value of capacity increases with K and is irrelevant to $\boldsymbol{a_t}$ because the transmit energy is mainly allocated to communication.

We also compared the runtime of solving the optimization using CVX and the analytical solutions given in Section 4. Performed on a personal computer with Intel (R) Core (TM) i7-9750H CPU @ 2.60 GHz and 16.0 GB RAM. The average runtime is given in Table 1. The results show that by using the analytical solutions in this work, the time consumption of solving the problem is significantly reduced.

6. Conclusion

In this paper, we consider a simplified scenario of a MIMO DFRC system where there is only one downlink user and one radar target. We take achievable communication rate as the communication performance metric and radar SNR as the radar performance metric. By constraining radar performance and optimizing communication performance, we formulate an optimization problem to study the performance bound of the system. Through theoretical analysis, we provide properties of the optimal transmit covariance matrix. Then, in the situation where the downlink user has only one receive antenna, we find the analytical expressions of the optimal waveform design and corresponding channel capacity. When the transmit steering vector is either parallel to one of the right-singular vectors of the channel matrix or orthogonal to the row space of the channel matrix, we also provide analytical solutions to the problem. The analysis and solutions show that the DFRC system essentially shares and allocates transmit power between radar target and downlink users, reveal the performance tradeoff between these two functions and facilitate the discussion on the performance bound of MIMO DFRC systems.

Appendix

A. Proof of Theorem 1

Inspired by the derivation in [29], we prove Theorem 1 mainly by assuming there is an optimal solution with rank r first and then discussing whether we can construct a new optimal solution with lower rank.

If the feasible set of the optimization problem (Equation (26)) is bounded and closed, an optimal solution of Equation (26) must exist. Suppose that there is an optimal solution $\boldsymbol{R}_0$ whose rank is r. Perform an eigenvalue decomposition on $\boldsymbol{R}_0$:

$$\boldsymbol{R}_0=\boldsymbol{U}\Lambda\boldsymbol{U}^H=\sum_{i=1}^{r}\lambda_i\boldsymbol{u}_i\boldsymbol{u}_i^H=\sum_{i=1}^{r}\boldsymbol{v}_i\boldsymbol{v}_i^H=\boldsymbol{V}\boldsymbol{V}^H, \tag{A.1}$$

where $\boldsymbol{v}_i=\sqrt{\lambda_i}\boldsymbol{u}_i\ (i=1,2,\cdots,r)$, $\boldsymbol{V}\in\mathbb{C}^{M\times r}$. Construct the matrix

$$\boldsymbol{R}_\alpha=\boldsymbol{V}(\boldsymbol{I}+\alpha\Delta)\boldsymbol{V}^H, \tag{A.2}$$

where $\Delta\in\mathbb{C}^{r\times r}$ is a Hermitian matrix.

Assume that Δ satisfies the following:

$$\begin{cases}\boldsymbol{H}\boldsymbol{V}\Delta\boldsymbol{V}^H\boldsymbol{H}^H=\boldsymbol{0},\\ \mathrm{tr}(\boldsymbol{Q}_i\boldsymbol{V}\Delta\boldsymbol{V}^H)=0,\ i=1,2,\cdots,n.\end{cases} \tag{A.3}$$

According to Equation (A.3),

$$\begin{aligned}\log|\boldsymbol{I}+\boldsymbol{H}\boldsymbol{R}_\alpha\boldsymbol{H}^H|&=\log|\boldsymbol{I}+\boldsymbol{H}\boldsymbol{V}(\boldsymbol{I}+\alpha\Delta)\boldsymbol{V}^H\boldsymbol{H}^H|\\&=\log|\boldsymbol{I}+\boldsymbol{H}\boldsymbol{V}\boldsymbol{V}^H\boldsymbol{H}^H|\\&=\log|\boldsymbol{I}+\boldsymbol{H}\boldsymbol{R}_0\boldsymbol{H}^H|.\end{aligned} \tag{A.4}$$

The value of the objective function remains the same when we change the value of the optimization variable from $\boldsymbol{R}_0$ to $\boldsymbol{R}_\alpha$. According to Equation (A.3),

$$\begin{aligned}\mathrm{tr}(\boldsymbol{Q}_i\boldsymbol{R}_\alpha)&=\mathrm{tr}(\boldsymbol{Q}_i\boldsymbol{V}(\boldsymbol{I}+\alpha\Delta)\boldsymbol{V}^H)\\&=\mathrm{tr}(\boldsymbol{Q}_i\boldsymbol{V}\boldsymbol{V}^H)\\&=\mathrm{tr}(\boldsymbol{Q}_i\boldsymbol{R}_0),\ i=1,2,\cdots,n,\end{aligned} \tag{A.5}$$

which means all the constraints hold for $\boldsymbol{R}_\alpha$. Therefore, $\boldsymbol{R}_\alpha$ is also an optimal solution to Equation (26) as long as it satisfies Equation (A.3).

Take the real and imaginary parts of each element in Δ as a real variable. Since Δ is Hermitian, there are r^2 real variables in Δ in total. According to Theorem 1, the rank of $\boldsymbol{H}$ is k; thus, Equation (A.3) is equivalent to k^2 real linear equations, and Equation (A.3) is equivalent to k^2+n real linear equations with all the constant terms equal to 0. If $r^2>k^2+n$, then the equation set (Equation (A.3)) has a non-zero solution $\Delta_0 \neq 0$. Denote the eigenvalue with the largest absolute value of Δ_0 as λ_0, and let

$$\alpha = -\frac{1}{\lambda_0}. \tag{A.6}$$

In this case, $\boldsymbol{R}_\alpha \succeq 0$ and rank $(\boldsymbol{R}_\alpha) \leq r-1$.

In conclusion, if there is an optimal solution to Equation (26) with rank r and $r^2>k^2+n$, then there must be an optimal solution whose rank is no more than $r-1$. Therefore, Equation (26) has an optimal solution whose rank is no more than r, where r satisfies as follows:

$$r^2 \leq k^2+n<(r+1)^2. \tag{A.7}$$

If we change some of the equality constraints into inequality constraints, the conclusion remains true, as can be proved in a similar manner.

B. Solving the optimization (Equation (38))

Before solving Equation (38), we analyze the feasibility of the optimization problem. According to Equation (38c), we have

$$\boldsymbol{a}_t^H \boldsymbol{c}\boldsymbol{c}^H \boldsymbol{a}_t \leq \|\boldsymbol{c}\|_2^2 \|\boldsymbol{a}_t\|_2^2 = P\|\boldsymbol{a}_t\|_2^2, \tag{B.1}$$

where the equality is achieved when $\boldsymbol{c}$ is parallel to $\boldsymbol{a}_t$. Thus, γ in Equation (38b) must satisfy the following:

$$\gamma \leq P\|\boldsymbol{a}_t\|_2^2. \tag{B.2}$$

Otherwise, there is no feasible solution for Equation (38), which proves the result of case (iii) in Section 4.1.1.

Since Equation (38) satisfies Slater's condition, we solve it by considering its KKT conditions. The Lagrange function of Equation (38) is given by the following:

$$\begin{aligned} &L(\boldsymbol{c}, \boldsymbol{c}^*, \lambda, \mu) \\ &= -\boldsymbol{h}^H \boldsymbol{c}\boldsymbol{c}^H \boldsymbol{h} + \lambda(\gamma - \boldsymbol{a}_t^H \boldsymbol{c}\boldsymbol{c}^H \boldsymbol{a}_t) + \mu(\mathrm{tr}(\boldsymbol{c}\boldsymbol{c}^H) - P), \end{aligned} \tag{B.3}$$

where λ and μ are dual variables. Then, its KKT conditions are as follows:

$$\begin{cases} \dfrac{\partial L(\boldsymbol{c}, \boldsymbol{c}^*, \lambda, \mu)}{\partial \boldsymbol{c}^*} = -\boldsymbol{h}^H \boldsymbol{c}\boldsymbol{h} - \lambda \boldsymbol{a}_t^H \boldsymbol{c}\boldsymbol{a}_t + \mu \boldsymbol{c} = \boldsymbol{0}, \\ \mathrm{tr}(\boldsymbol{c}\boldsymbol{c}^H) - P = 0, \\ \gamma - \boldsymbol{a}_t^H \boldsymbol{c}\boldsymbol{c}^H \boldsymbol{a}_t \leq 0, \\ \lambda \geq 0, \\ \lambda(\gamma - \boldsymbol{a}_t^H \boldsymbol{c}\boldsymbol{c}^H \boldsymbol{a}_t) = 0. \end{cases} \tag{B.4}$$

Rewrite Equation (B.4) as follows:

$$\boldsymbol{c} = \frac{\boldsymbol{h}^H \boldsymbol{c}}{\mu}\boldsymbol{h} + \frac{\lambda \boldsymbol{a}_t^H \boldsymbol{c}}{\mu}\boldsymbol{a}_t, \tag{B.5}$$

To solve Equation (B.4), we need to calculate a and b in the assumption (Equation (37)) by substituting Equation (37) into Equation (B.4).

According to Equation (B.4), at least one of λ and $\gamma - \boldsymbol{a}_t^H \boldsymbol{c}\boldsymbol{c}^H \boldsymbol{a}_t$ equals 0. Consider the case that $\lambda = 0$. Then, Equation (B.5) becomes the following:

$$\boldsymbol{c} = \frac{\boldsymbol{h}^H \boldsymbol{c}}{\mu}\boldsymbol{h}. \tag{B.6}$$

Substituting Equation (37) into Equations (B.4) and (B.6) yields the following:

$$\begin{cases} |a|^2 \boldsymbol{h}^H \boldsymbol{h} + a^* b \boldsymbol{h}^H \boldsymbol{a}_t + a b^* \boldsymbol{a}_t^H \boldsymbol{h} + |b|^2 \boldsymbol{a}_t^H \boldsymbol{a}_t = P, \\ a\boldsymbol{h} + b\boldsymbol{a}_t = \dfrac{a\boldsymbol{h}^H \boldsymbol{h} + b\boldsymbol{h}^H \boldsymbol{a}_t}{\mu}\boldsymbol{h}. \end{cases} \tag{B.7}$$

According to Equation (B.7), we find that

$$b = 0. \tag{B.8}$$

By substituting Equation (B.8) into Equation (B.7), we obtain that

$$|a| = \frac{\sqrt{P}}{\|\boldsymbol{h}\|_2}, \tag{B.9}$$

where the phase of a is arbitrary. Substitute the solution of $\boldsymbol{c}$ into Equation (B.4). We then find that

$$\gamma \leq \frac{P|\boldsymbol{h}^H \boldsymbol{a}_t|^2}{\|\boldsymbol{h}\|_2^2}, \tag{B.10}$$

which proves the result of case (i) in Section 4.1.1.

Next, consider the case that

$$\gamma - \boldsymbol{a}_t^H \boldsymbol{c}\boldsymbol{c}^H \boldsymbol{a}_t = 0. \tag{B.11}$$

By substituting Equation (37), we rewrite Equations (B.11) and (B.5) as follows:

$$\begin{cases} |a|^2 \boldsymbol{a}_t^H \boldsymbol{h}\boldsymbol{h}^H \boldsymbol{a}_t + a^* b \boldsymbol{a}_t^H \boldsymbol{a}_t \boldsymbol{h}^H \boldsymbol{a}_t \\ \quad + a b^* \boldsymbol{a}_t^H \boldsymbol{h} \boldsymbol{a}_t^H \boldsymbol{a}_t + |b|^2 \boldsymbol{a}_t^H \boldsymbol{a}_t \boldsymbol{a}_t^H \boldsymbol{a}_t = \gamma, \\ a\boldsymbol{h} + b\boldsymbol{a}_t \\ \quad = \dfrac{a\boldsymbol{h}^H \boldsymbol{h} + b\boldsymbol{h}^H \boldsymbol{a}_t}{\mu} \boldsymbol{h} + \dfrac{\lambda(a\boldsymbol{a}_t^H \boldsymbol{h} + b\boldsymbol{a}_t^H \boldsymbol{a}_t)}{\mu} \boldsymbol{a}_t. \end{cases} \tag{B.12}$$

Combining Equations (B.7) and (B.12), we obtain that

$$|a| = \eta := \sqrt{\frac{P\|\boldsymbol{a}_t\|_2^2 - \gamma}{\|\boldsymbol{h}\|_2^2 \|\boldsymbol{a}_t\|_2^2 - |\boldsymbol{h}^H \boldsymbol{a}_t|^2}}. \tag{B.13}$$

From Equation (B.12), we find the relationship between the phases of a and b:

$$\begin{cases} \arg(a) = \arg(a\boldsymbol{h}^H \boldsymbol{h} + b\boldsymbol{h}^H \boldsymbol{a}_t), \\ \arg(b) = \arg(a\boldsymbol{a}_t^H \boldsymbol{h} + b\boldsymbol{a}_t^H \boldsymbol{a}_t). \end{cases} \tag{B.14}$$

When $\boldsymbol{h}^H \boldsymbol{a}_t = 0$, Equation (B.14) always holds, and the phases of a and b are arbitrary. When $\boldsymbol{h}^H \boldsymbol{a}_t \neq 0$, we have the following:

$$\arg(a) - \arg(b) = \arg(\boldsymbol{h}^H \boldsymbol{a}_t). \tag{B.15}$$

This results from the facts that $\boldsymbol{h}^H \boldsymbol{h}$ in Equation (B.14) is a real number and $\arg(a) = \arg(a\boldsymbol{h}^H \boldsymbol{h})$, which implies $\arg(a) = \arg(b\boldsymbol{h}^H \boldsymbol{a}_t)$. Similarly, $\arg(b) = \arg(a\boldsymbol{a}_t^H \boldsymbol{h})$.

Substituting Equation (B.13) and the relationship between the phases of a and b into Equation (B.7) yields the following:

$$|b| = \frac{\sqrt{\gamma}}{\|\boldsymbol{a}_t\|_2^2} - \frac{|\boldsymbol{h}^H \boldsymbol{a}_t|}{\|\boldsymbol{a}_t\|_2^2} \eta. \tag{B.16}$$

In addition, since $|b| \geq 0$, we have $\gamma \geq \frac{P|\boldsymbol{h}^H \boldsymbol{a}_t|^2}{\|\boldsymbol{h}\|_2^2}$. From Equations (B.13), (B.15), and (B.16), we prove the result of case (ii) in Section 4.1.1.

C. Solving the optimization (Equation (14)) under the situation of Section 4.2

To better depict the relationship between $\boldsymbol{a}_t$ and $\boldsymbol{H}$, we first perform a singular value decomposition (SVD) on the channel matrix $\boldsymbol{H}$:

$$\boldsymbol{H} = \boldsymbol{U}_{\boldsymbol{H}} \Sigma \boldsymbol{V}_{\boldsymbol{H}}^H, \tag{C.1}$$

where

$$\Sigma \boldsymbol{V}_{\boldsymbol{H}}^H = [\, h_1 \boldsymbol{e}_1 \quad h_2 \boldsymbol{e}_2 \quad \cdots \quad h_K \boldsymbol{e}_K \,]^H, \tag{C.2}$$

$h_1, h_2, \cdots, h_K$ are the singular values of $\boldsymbol{H}$ and $\boldsymbol{e}_1, \boldsymbol{e}_2, \cdots, \boldsymbol{e}_K \in \mathbb{C}^M$ are the corresponding right-singular vectors.

Substituting Equation (C.1) into the objective function (Equation (14a)) yields the following:

$$\begin{aligned} \log|\boldsymbol{I}_K + \boldsymbol{H}\boldsymbol{R}\boldsymbol{H}^H| &= \log|\boldsymbol{U}\boldsymbol{U}^H + \boldsymbol{U}\Sigma \boldsymbol{V}^H \boldsymbol{R} \boldsymbol{V} \Sigma^H \boldsymbol{U}^H| \\ &= \log|\boldsymbol{I}_K + \Sigma \boldsymbol{V}^H \boldsymbol{R} \boldsymbol{V} \Sigma^H|. \end{aligned} \tag{C.3}$$

Using the assumption $\boldsymbol{R} = \boldsymbol{C}\boldsymbol{C}^H$ in the proof of Proposition 3, we rewrite the optimization problem (Equation (14)) as follows:

$$\max_{\boldsymbol{C}} \ \log|\boldsymbol{I}_K + \Sigma \boldsymbol{V}^H \boldsymbol{C}\boldsymbol{C}^H \boldsymbol{V} \Sigma^H|, \tag{C.4a}$$

$$\text{s.t.} \ \ \boldsymbol{a}_t^H \boldsymbol{C}\boldsymbol{C}^H \boldsymbol{a}_t \geq \gamma, \tag{C.4b}$$

$$\operatorname{tr}(\boldsymbol{C}\boldsymbol{C}^H) = P. \tag{C.4c}$$

The KKT conditions of Equation (C.4) give that

$$\begin{cases} \dfrac{\partial L(\boldsymbol{C}, \boldsymbol{C}^*, \lambda, \mu)}{\partial \boldsymbol{C}^*} = 0, \\ \operatorname{tr}(\boldsymbol{C}\boldsymbol{C}^H) - P = 0, \end{cases} \tag{C.5}$$

where

$$\begin{aligned} &\frac{\partial L(\boldsymbol{C}, \boldsymbol{C}^*, \lambda, \mu)}{\partial \boldsymbol{C}^*} \\ &= -\boldsymbol{V}_{\boldsymbol{H}} \Sigma^H (\boldsymbol{I} + \Sigma \boldsymbol{V}_{\boldsymbol{H}}^H \boldsymbol{C}\boldsymbol{C}^H \boldsymbol{V}_{\boldsymbol{H}} \Sigma^H)^{-1} \Sigma \boldsymbol{V}_{\boldsymbol{H}}^H \boldsymbol{C} \\ &\quad - \lambda \boldsymbol{a}_t \boldsymbol{a}_t^H \boldsymbol{C} + \mu \boldsymbol{C}, \end{aligned} \tag{C.6}$$

and λ, μ are dual variables.

C.1 When $\boldsymbol{a}_t$ Is Parallel to One of the Right-Singular Vectors of $\boldsymbol{H}$. Without loss of generality, assume that $\boldsymbol{a}_t$ is parallel to $\boldsymbol{e}_1$

$$\boldsymbol{a}_t = a\boldsymbol{e}_1. \tag{C.7}$$

Inspired by the derivation in [25] and the properties provided in Section 3, we speculate that in this situation the rank of the optimal transmit covariance matrix $\boldsymbol{R}$ equals that of $\boldsymbol{H}$ and the eigenvectors of $\boldsymbol{R}$ are parallel to the right-singular vectors of $\boldsymbol{H}$. Thus the optimal $\boldsymbol{C}$ can be expressed as follows:

$$\boldsymbol{C} = [\, c_1 \boldsymbol{e}_1 \quad c_2 \boldsymbol{e}_2 \quad \cdots \quad c_K \boldsymbol{e}_K \quad 0 \quad \cdots \quad 0 \,]. \tag{C.8}$$

First, we consider the case in which $\gamma - \boldsymbol{a}_t^H \boldsymbol{C}\boldsymbol{C}^H \boldsymbol{a}_t < 0$. In this case, the radar SNR constraint (Equation (C.4b)) is inactive. Thus the optimal solution is obtained by solving Equation (C.4) without regard to Equation (C.4b), in which

$|c_1|^2, |c_2|^2, \cdots, |c_K|^2$ are obtained by utilizing the water-filling algorithm [25].

If the optimal solution obtained in this way does not satisfy that $\gamma - \boldsymbol{a}_t^H \boldsymbol{C}\boldsymbol{C}^H \boldsymbol{a}_t < 0$, then there must be the following:

$$\gamma - \boldsymbol{a}_t^H \boldsymbol{C}\boldsymbol{C}^H \boldsymbol{a}_t = 0. \tag{C.9}$$

Substituting Equations (C.7) and (C.8) into Equation (C.9) and solving the equation we have the following:

$$|c_1|^2 = \frac{\gamma}{|a|^2}. \tag{C.10}$$

Combining Equations (C.8), (C.8), and (C.5), the KKT conditions are rewritten as follows:

$$\begin{cases} [\, a_1\boldsymbol{e}_1 \quad a_2\boldsymbol{e}_2 \quad \cdots \quad a_K\boldsymbol{e}_K \,] = \boldsymbol{0}, \\ \sum\limits_{i=2}^{K} |c_i|^2 = P - |c_1|^2 = P - \dfrac{\gamma}{|a|^2}, \end{cases} \tag{C.11}$$

where $a_1, a_2, \cdots, a_K$ are given by the following:

$$a_i = \begin{cases} \left(\mu - \lambda - \dfrac{|h_i|^2}{1 + |h_i|^2 |c_i|^2}\right) c_i, & i = 1, \\ \left(\mu - \dfrac{|h_i|^2}{1 + |h_i|^2 |c_i|^2}\right) c_i, & i = 2, 3, \cdots, K. \end{cases} \tag{C.12}$$

According to Equations (C.11) and (C.12), $|c_2|^2, |c_3|^2, \cdots, |c_K|^2$ are solved by using the water-filling algorithm:

$$|c_i|^2 = \max\left(\frac{1}{\mu} - \frac{1}{|h_i|^2},\, 0\right),\ i = 2, 3, \cdots, K. \tag{C.13}$$

The dual variables λ and μ are solved by substituting Equations (C.10), (C.12), and (C.13) into Equation (C.11).

In conclusion, the optimal transmit covariance matrix is as follows

$$\boldsymbol{R} = \boldsymbol{C}\boldsymbol{C}^H = \sum_{i=1}^{K} |c_i|^2 \boldsymbol{e}_i \boldsymbol{e}_i^H, \tag{C.14}$$

where $|c_1|^2, |c_2|^2, \cdots, |c_K|^2$ are given by previous derivation.

C.2 When $\boldsymbol{a}_t$ Is Orthogonal to the Row Space of $\boldsymbol{H}$. Assume that

$$\boldsymbol{e}_{K+1} = \frac{\boldsymbol{a}_t}{|\boldsymbol{a}_t|}, \tag{C.15}$$

and the optimal $\boldsymbol{C}$ is in the form of

$$\boldsymbol{C} = [\, c_1\boldsymbol{e}_1 \quad \cdots \quad c_K\boldsymbol{e}_K \quad c_{K+1}\boldsymbol{e}_{K+1} \,]. \tag{C.16}$$

Similar to the derivation in Section C.1, the KKT conditions are rewritten as follows:

$$\begin{cases} [\, a_1\boldsymbol{e}_1 \quad a_2\boldsymbol{e}_2 \quad \cdots \quad a_{K+1}\boldsymbol{e}_{K+1} \,] = \boldsymbol{0}, \\ \sum\limits_{i=1}^{K} |c_i|^2 = P - |c_{K+1}|^2 = P - \dfrac{\gamma}{|a|^2}, \end{cases} \tag{C.17}$$

where

$$a_i = \begin{cases} \left(\mu - \dfrac{|h_i|^2}{1 + |h_i|^2 |c_i|^2}\right) c_i, & i = 1, 2, \cdots, K, \\ (\mu - \lambda |\boldsymbol{a}_t|^2) c_i, & i = K + 1. \end{cases} \tag{C.18}$$

Solving the KKT conditions, we obtain that the optimal transmit covariance matrix is given by the following:

$$\boldsymbol{R} = \boldsymbol{C}\boldsymbol{C}^H = \sum_{i=1}^{K+1} |c_i|^2 \boldsymbol{e}_i \boldsymbol{e}_i^H, \tag{C.19}$$

where

$$|c_{K+1}|^2 = \frac{\gamma}{|\boldsymbol{a}_t|^2}, \tag{C.20}$$

and

$$|c_i|^2 = \max\left(\frac{1}{\mu} - \frac{1}{|h_i|^2},\, 0\right),\ i = 1, 2, \cdots, K. \tag{C.21}$$

The dual variables λ and μ are solved by substituting Equations (C.18), (C.20), and (C.21) into Equation (C.17).

Although we assumed the form of the optimal transmit covariance matrix in the derivation, the optimal solutions we obtained in Sections C.1 and C.2 satisfy the original KKT conditions, which means the results are exactly the optimal solution under the corresponding cases. In addition, the optimal solutions we obtained in these two cases conform to the properties we provided in Section 3.

Data Availability

No underlying data were collected or produced in this study.

Disclosure

A preprint has previously been published [30].

Conflicts of Interest

The authors declare that they have no conflicts of interest.

Acknowledgments

This work was supported by the National Natural Science Foundation of China under grant no. 62171259.

References

[1] A. Hassanien, M. G. Amin, Y. D. Zhang, and F. Ahmad, "Signaling strategies for dual-function radar communications: an overview," *IEEE Aerospace and Electronic Systems Magazine*, vol. 31, no. 10, pp. 36–45, 2016.

[2] J. Qian, M. Lops, L. Zheng, X. Wang, and Z. He, "Joint system design for coexistence of MIMO radar and MIMO communication," *IEEE Transactions on Signal Processing*, vol. 66, no. 13, pp. 3504–3519, 2018.

[3] J. Qian, Z. He, N. Huang, and B. Li, "Transmit designs for spectral coexistence of MIMO radar and MIMO communication systems," *IEEE Transactions on Circuits and Systems II: Express Briefs*, vol. 65, no. 12, pp. 2072–2076, 2018.

[4] J. Qian, L. Venturino, M. Lops, and X. Wang, "Radar and communication spectral coexistence in range-dependent interference," *IEEE Transactions on Signal Processing*, vol. 69, pp. 5891–5906, 2021.

[5] A. R. Chiriyath, B. Paul, G. M. Jacyna, and D. W. Bliss, "Inner bounds on performance of radar and communications coexistence," *IEEE Transactions on Signal Processing*, vol. 64, no. 2, pp. 464–474, 2016.

[6] D. Ma, N. Shlezinger, T. Huang, Y. Liu, and Y. C. Eldar, "Joint radar-communication strategies for autonomous vehicles: combining two key automotive technologies," *IEEE Signal Processing Magazine*, vol. 37, no. 4, pp. 85–97, 2020.

[7] L. Zheng, M. Lops, Y. C. Eldar, and X. Wang, "Radar and communication coexistence: an overview: a review of recent methods," *IEEE Signal Processing Magazine*, vol. 36, no. 5, pp. 85–99, 2019.

[8] F. Liu, Y. Cui, C. Masouros et al., "Integrated sensing and communications: toward dual-functional wireless networks for 6G and beyond," *IEEE Journal on Selected Areas in Communications*, vol. 40, no. 6, pp. 1728–1767, 2022.

[9] C. Sturm and W. Wiesbeck, "Waveform design and signal processing aspects for fusion of wireless communications and radar sensing," *Proceedings of the IEEE*, vol. 99, pp. 1236–1259, 2011.

[10] J. Moghaddasi and K. Wu, "Multifunctional transceiver for future radar sensing and radio communicating data-fusion platform," *IEEE Access*, vol. 4, pp. 818–838, 2016.

[11] X. Liu, Y. Liu, X. Wang, and J. Zhou, "Application of communication OFDM waveform to SAR imaging," in *2017 IEEE Radar Conference (RadarConf)*, pp. 1757–1760, IEEE, Seattle, WA, USA, 2017.

[12] Y. Zhang, Q. Li, L. Huang, C. Pan, and J. Song, "A modified waveform design for radar-communication integration based on LFM-CPM," in *2017 IEEE 85th Vehicular Technology Conference (VTC Spring)*, pp. 1–5, IEEE, Sydney, NSW, Australia, 2017.

[13] X. Liu, T. Huang, N. Shlezinger, Y. Liu, J. Zhou, and Y. C. Eldar, "Joint transmit beamforming for multiuser MIMO communications and MIMO radar," *IEEE Transactions on Signal Processing*, vol. 68, pp. 3929–3944, 2020.

[14] E. Fishler, A. Haimovich, R. S. Blum, L. J. Cimini, D. Chizhik, and R. A. Valenzuela, "Spatial diversity in radars—models and detection performance," *IEEE Transactions on Signal Processing*, vol. 54, no. 3, pp. 823–838, 2006.

[15] J. G. Andrews, S. Buzzi, W. Choi et al., "What will 5G be?" *IEEE Journal on Selected Areas in Communications*, vol. 32, no. 6, pp. 1065–1082, 2014.

[16] X. Liu, T. Huang, Y. Liu, and J. Zhou, "Achievable sum-rate capacity optimization for joint MIMO multiuser communications and radar," in *2021 IEEE 22nd International Workshop on Signal Processing Advances in Wireless Communications (SPAWC)*, pp. 466–470, IEEE, Lucca, Italy, 2021.

[17] C. Sahin, J. Jakabosky, P. M. McCormick, J. G. Metcalf, and S. D. Blunt, "A novel approach for embedding communication symbols into physical radar waveforms," in *2017 IEEE Radar Conference (RadarConf)*, pp. 1498–1503, IEEE, Seattle, WA, USA, 2017.

[18] E. Telatar, "Capacity of multi-antenna Gaussian channels," *European Transactions on Telecommunications*, vol. 10, no. 6, pp. 585–595, 1999.

[19] T. M. Pham, "On the MIMO capacity with multiple power constraints," Maynooth University Department of Electronic Engineering. United States, 2020.

[20] M. Vu, "MISO capacity with per-antenna power constraint," *IEEE Transactions on Communications*, vol. 59, no. 5, pp. 1268–1274, 2011.

[21] B. Tang, Z. Huang, L. Qin, and H. Wang, "Fundamental limits on detection with a dual-function radar communication system," in *2021 CIE International Conference on Radar (Radar)*, pp. 2862–2866, IEEE, Haikou, Hainan, China, 2021.

[22] L. Chen, Z. Wang, Y. Du, Y. Chen, and F. R. Yu, "Generalized transceiver beamforming for DFRC with MIMO radar and MU-MIMO communication," *IEEE Journal on Selected Areas in Communications*, vol. 40, no. 6, pp. 1795–1808, 2022.

[23] B. Tang and P. Stoica, "MIMO multifunction rf systems: detection performance and waveform design," *IEEE Transactions on Signal Processing*, vol. 70, pp. 4381–4394, 2022.

[24] S. Imani, S. A. Ghorashi, and M. Bolhasani, "SINR maximization in colocated MIMO radars using transmit covariance matrix," *Signal Processing*, vol. 119, pp. 128–135, 2016.

[25] L. Vandenberghe, S. Boyd, and S. P. Wu, "Determinant maximization with linear matrix inequality constraints," *Siam Journal on Matrix Analysis & Applications*, vol. 19, no. 2, pp. 499–533, 1998.

[26] M. Grant and S. Boyd, "CVX: matlab software for disciplined convex programming, version 2.1," 2014, http://cvxr.com/cvx.

[27] M. Grant and S. Boyd, "Graph implementations for nonsmooth convex programs," in *Recent Advances in Learning and Control*, vol. 371 of *Lecture Notes in Control and Information Sciences*, pp. 95–110, Springer, London, 2008.

[28] T. J. Richardson, M. A. Shokrollahi, and R. L. Urbanke, "Design of capacity-approaching irregular low-density parity-check codes," *IEEE Transactions on Information Theory*, vol. 47, no. 2, pp. 619–637, 2001.

[29] G. Pataki, "On the rank of extreme matrices in semidefinite programs and the multiplicity of optimal eigenvalues," *Mathematics of Operations Research*, vol. 23, no. 2, pp. 339–358, 1998.

[30] Z. Zheng, X. Liu, T. Huang, Y. Liu, and Y. C. Eldar, "Towards a performance bound on MIMO DFRC systems," arXiv preprint arXiv: 221106979, 2022.